Title

Read-out Segmented Echo Planar Imaging with Two-Dimensional Navigator Correction (RESOLVE): An Alternative Sequence to Improve Image Quality on Diffusion-Weighted Imaging of Prostate.

Journal

British Journal of Radiology, 95(1136)

Authors

Felker, Ely
Suvannarerg, Voraparee
Tubtawee, Teeravut
et al.

Publication Date

2022-08-01

DOI

10.1259/bjr.20211165

Peer reviewed

BJR

https://doi.org/10.1259/bjr.20211165

Received: 19 October 2021 | Revised: 28 April 2022 | Accepted: 23 May 2022 | Published online: 22 June 2022

Cite this article as:
Hosseiny M, Sung KH, Felker E, Suvannarerg V, Tubtawee T, Shafa A, et al. Read-out Segmented Echo Planar Imaging with Two-Dimensional Navigator Correction (RESOLVE): An Alternative Sequence to Improve Image Quality on Diffusion-Weighted Imaging of Prostate. *Br J Radiol* (2022) 10.1259/bjr.20211165.

FULL PAPER

Read-out Segmented Echo Planar Imaging with Two-Dimensional Navigator Correction (RESOLVE): An Alternative Sequence to Improve Image Quality on Diffusion-Weighted Imaging of Prostate

[1]MELINA HOSSEINY, MD, [1]KYUNG HYUN SUNG, PhD, [1]ELY FELKER, MD, [1]VORAPAREE SUVANNARERG, MD, [1,2]TEERAVUT TUBTAWEE, MD, [1]ARIEL SHAFA, [1]KRISHAN R. ARORA, [1]JUSTIN CHING, [1]ANJALIE GULATI, [1]AFSHIN AZADIKHAH, MD, [3]XIAODONG ZHONG, [4]JAMES SAYRE, [1]DAVID LU, MD and [1,5]STEVEN S RAMAN, MD

[1]Department of Radiology, Ronald Reagan-UCLA Medical Center, David Geffen School of Medicine at UCLA, Los Angeles, California, United States
[2]Department of Radiology, Prince of Songkla University, Hat Yai, Songkhla, Thailand
[3]Siemens Healthcare, MR R&D Collaborations, Lilburn, Georgia, United States
[4]Department of Bioinformatics, David Geffen School of Medicine at UCLA, Los Angeles, California, United States
[5]Department of Urology, Ronald Reagan-UCLA Medical Center, David Geffen School of Medicine at UCLA, Los Angeles, California, United States

Address correspondence to: Dr Melina Hosseiny
E-mail: *melina2.hosseiny@gmail.com*

Objective: We aimed to investigate if the use of read-out segmented echoplanar imaging with additional two-dimensional navigator correction (Readout Segmentation of Long Variable Echo, RESOLVE) for acquiring prostate diffusion-weighted imaging (DWI) improves image quality, compared to single-shot echoplanar imaging (ss-EPI).

Methods: This single-center prospective study cohort included 162 males with suspected prostate cancer, who underwent 3 Tesla multiparametric MRI (3T-mpMRI). Two abdominal radiologists, blinded to the clinical information, separately reviewed each 3T-mpMRI study to rank geometrical distortion, degree of rectal distention, lesion conspicuity, and anatomic details delineation first on ss-EPI-DWI and later on RESOLVE-DWI using 5-point scales (1 = excellent, 5 = poor). The average of the ranking scores given by two readers was generated and used as the final score.

Results: There was good-to-excellent interreader agreement for scoring image quality parameters on both ss-EPI and RESOLVE. Geometrical distortion scores > 3 was seen in 12.3% (20/162) of ss-EPI images, with all having geometrical distortion score <3 on RESOLVE (p < .001). The mean image distortion score was significantly less on RESOLVE than ss-EPI (1.16 *vs* 1.61, p < .01 regardless of rectal gas, p< .05 when stratified by the degree of rectal distention). RESOLVE was superior to ss-EPI for lesion conspicuity (mean 1.35 *vs* 1.53, p< .002) and anatomic delineation (2.60 *vs* 2.68, p< .001) of prostate on DWI.

Conclusion: Compared to conventional ss-EPI, the use of RESOLVE for acquisition of prostate DWI resulted in significantly enhanced image quality and reduced geometrical distortion.

Advances in knowledge: RESOLVE could be an alternative or replacement of ss-EPI for acquiring prostate DWI with significantly less geometrical distortion and significantly improved lesion conspicuity and anatomic delineation.

INTRODUCTION

Prostate cancer is the second leading cause of cancer-related mortality in males and is the only solid organ cancer not routinely imaged prior to biopsy.[1] 3 Tesla multiparametric MRI (3T-mpMRI) is currently the non-invasive imaging of choice for detection, localization, and characterization of the prostate cancer (PCa) lesions with improved biopsy yield and surgical outcomes.[2–4] Diffusion-weighted imaging (DWI) is considered the primary sequence in the peripheral zone (PZ) and secondary sequence in transition zone (TZ) for detection of PCa according to ACR-ESUR PIRADS v. 2.1 guidelines, which also suggest DWI acquisition using single-shot echoplanar imaging (ss-EPI) technique.[5] ss-EPI is highly sensitive to MR-susceptibility artifacts, which may

lead to geometrical distortion and image blurring. The susceptibility artifacts occur near the boundaries of tissues with different magnetic susceptibility such as air–soft tissue interfaces. The susceptibility artifact increases exponentially at higher magnetic fields.[6,7] Given the close proximity of the PZ to the rectum, distortion from artifacts on DWI can significantly hinder the evaluation of PZ lesions and impair the identification of target lesions. A significant increase in the severity of DWI geometric distortion is observed with an increment in the degree of rectal distension.[8] As an essential sequence in the mpMRI of prostate cancer, it is essential to optimize the image quality of DWI.

Readout-segmented echoplanar imaging (rs-EPI) is an alternative sequence for obtaining DWI.[9,10] Initial studies have found a significant increase in image quality using rs-EPI.[11–18] In rs-EPI, k-space is partitioned into several adjacent segments, or "blinds", along the readout-encoding direction in each shot, which allows marked decrement in echo spacing, T2* blurring, MR susceptibility artifact and geometrical distortion.[9] Readout Segmentation of Long Variable Echo (RESOLVE) is a type of rs-EPI technique with additional two-dimensional navigator correction to robustly correct motion-induced phase errors,[10] and has been reported to improve susceptibility sensitivity, reduce image distortion and improve image quality for lesion detection and delineation.[12,19–23] The purpose of this study was to compare the image quality in RESOLVE DWI to standard ss-EPI DWI on the prostate 3T-mpMRI. We aimed to qualitatively assess the possible benefits of acquiring RESOLVE DWI in decreasing geometrical distortion and improving the image quality.

METHODS AND MATERIALS

Study design

This single-center, 1996 Health Insurance Portability and Accountability Act (HIPAA)-compliant, and institutional review board (IRB)-approved single-arm prospective study was performed with a waiver of the informed consent at David Geffen School of Medicine at University of California, Los Angeles (UCLA). The study cohort initially comprised 180 consecutive patients who underwent 3T mpMRI for suspected prostate cancer between January and April 2019. All participants had undergone 3T mpMRI of the prostate based on the institution criteria, including clinically suspected prostate cancer, abnormality in transrectal ultrasound-guided biopsy, or clinical suspicion of PCa despite negative biopsy. Patients with history of prior prostate or other pelvic surgery, radiation therapy or those with incomplete MRI assessment were excluded. The final study cohort comprised 162 men with a mean age of 69 years (range 59–84 years), mean PSA 7.4 ng ml^{-1} (range 0.6–35.5 ng ml^{-1}) and mean prostate volume of 58.9 cc (range 52–163 cc), at the time of acquiring MRI. In 85/162 of the patients, a prostate lesion was seen on prostate MRI and lesion conspicuity was scored in their MRI.

MRI protocol

Multiparametric MR imaging of the prostate was performed on a single 3T scanner (MAGNETOM Skyra, Siemens Healthcare, Erlangen, Germany) with a pelvic external phased-array coil using the same standard protocol compliant with recommendations of ACR and ESUR. The protocol relevant to this study included two-dimensional turbo spin-echo (TSE) *T2*-weighted imaging three-dimensional dynamic contrast-enhanced (DCE) imaging (acquired in the axial plane and then reformatted in all three planes) and echoplanar diffusion-weighted imaging. DWI was obtained in all individuals using two sequences, ss-EPI and RESOLVE.

Because rs-EPI uses a readout-segmented EPI k-space trajectory and has different SNR efficiency from the ss-EPI,[10] we optimized the protocols of ss-EPI and rs-EPI separately according to the empirical abdominal imaging experience at our institution. Imaging parameters including field of view (FOV), pixel sizes, b-values, averages, repetition time (TR) and echo time (TE) were set with the intent to achieve the diagnostic image quality within the clinically accepted acquisition time, and not forced to be the same between these two sequences, as listed in Table 1.

Table 1. Imaging parameters of ss-EPI and rsEPI

Parameters	ss-EPI	rs-EPI (RESOLVE)
In-plane pixel size (mm^2)	1.6 × 1.6	2.0 × 2.0
FOV (mm)	260 × 153	220 × 220
Phase FOV (%)	82	100
TR (ms)	4800	4530
TE (ms)	80	57
Navigator echo acquired for distortion correction	No	Yes
k-space trajectory	ssEPI	rsEPI
Acquired b-values (s/mm^2)	0, 100, 400, 800	50, 800
Averages of acquired b-values	7, 7, 7, 7	1, 2
Calculated b-value (s/mm^2)	1400	1400
Acquisition time (min:s)	6:02	4:47

EPI, echoplanar imaging; FOV, field of view; RESOLVE, Readout Segmentation of Long Variable Echo; TE, echo time; TR, repetition time; rsEPI, readout-segmented EPI; ssEPI, single-shot EPI.

Image interpretation and definitions

Two abdominal radiologists (each with more than 15 years of experience in prostate imaging), blinded to the clinical information of patients, separately evaluated each anonymized MRI exam to rank geometrical distortion, lesion conspicuity, and anatomic delineation on a 5-point scale, first on ssEPI-DWI and with a 2-week interval on RESOLVE-DWI to minimize recall. The corresponding *T2*-weighted TSE images were used as the reference standard for delineating the prostate boundary and lesion depiction. The average of the ranking scores given by two readers was generated and used as the final score.

A 5-point Likert scale was used to rank the geometrical distortion on ss-EPI and RESOLVE as followed: 1: no perceptible artifact, 2: minimal susceptibility artifact, which did not interfere with diagnosis, 3: mild susceptibility artifact, obscuring <50% of the peripheral zone, 4: moderate susceptibility artifact, obscuring >50% of the peripheral zone, and 5: severe susceptibility artifact, affecting the peripheral and transitional zones. Geometrical distortion score of 3 or higher was considered as significant distortion.

The radiologists rated lesion conspicuity (contrast of the lesion to background tissue) and detailed anatomic delineation (defined as differentiation of PZ from TZ, delineation of urethra, visualization of the extent of a lesion) as well. The 5-point Likert scale for lesion conspicuity was as followed: 1: well-identified lesion with well-defined edges, 2: well-identified lesion with poor-defined edges, 3: lesion identified subtly with poor-defined edges, 4: differentiation between lesion and normal anatomy is not clear, 5: lesion unidentifiable on imaging.

Both axial and sagittal planes were used for manual anatomic delineation of the prostate gland and the following scoring system was used for this purpose: 1: excellent delineation with strong contrast to adjacent tissues, 2: clear delineation with relatively clear contrast to adjacent tissues, 3: intermediate delineation with moderate contrast to adjacent tissues, 4: difficult delineation with subtle contrast to adjacent tissues, 5: poor delineation with insufficient contrast to adjacent tissue.

The degree of rectal distention was also scored based on the largest transverse diameter in dynamic contrast-enhanced images using a 5-point scale as1: collapsed rectal wall, 2: minimal (<1 cm), 3: mild (1–2 cm), 4: moderate (2–3 cm) and 5: marked (>3 cm) volume of rectal gas.

All the MRI studies were earlier interpreted by other abdominal radiologists based on the PIRADS v. 2 guidelines and later patients with PIRADS scores 3–5 underwent MR-directed biopsy, with either fusion ultrasound-MR or in-bore MR-guided techniques.

Statistical analysis

A weighted κ test was used to measure the interreader variability. Non-parametric two-tailed Wilcoxon signed rank test was used to compare rankings between ss-EPI and RESOLVE. Binary logistic regression analysis was used to assess the association between rectal distention and mild-to-severe geometrical distortion on ss-EPI. The statistical significance level was set as two-tailed p-value < 0.05. All statistical analyses were performed using SPSS software v. 18 (IBM).

RESULTS

Interreader agreements

In the study cohort of 162 patients, the interreader agreement for scoring image distortion in ss-EPI and RESOLVE were 0.85 and 0.79, respectively (Figure 1). The interreader agreements for scoring lesion conspicuity and anatomic detail delineation were 0.87, and 0.77 in ss-EPI; and 0.74, and 0.79 in RESOLVE, respectively.

Geometrical distortion

In 26.5% (43/162) of 3T-mpMRI studies, mild-to-severe (score 3–5) rectal distention was detected. Higher degree of rectal distention was significantly associated with geometrical distortion (scores 3–5) on ss-EPI (OR: 3.07,95% CI: 1.90–4.97).

Of 162 MR scans, 20 (12.3%) had significant geometrical distortion on ss-EPI. None of these patients (0/20) had significant geometrical distortion on RESOLVE (p < .001). On head-to-head comparison of geometrical distortion scoring between ss-EPI and RESOLVE, less degree of geometrical distortion was observed in 42% of scans (68/162) on RESOLVE compared to ss-EPI (Figures 2 and 3 show examples of geometrical distortion in MR images). The mean DWI geometrical distortion scores were 1.61 and 1.16 on ss-EPI and RESOLVE, respectively. Geometrical distortion was significantly less on RESOLVE compared to ss-EPI, regardless of the rectal gas degree (p < .01) and when stratified by rectal distention scoring (p < .05).

Lesion conspicuity and anatomic delineation

In 85 prostate mpMRI with an identifiable lesion, the mean lesion conspicuity score was significantly improved on RESOLVE compared to ss-EPI (1.35 *vs* 1.53 p < .002). Lesion contrast was better on RESOLVE than ss-EPI in 23.5% (20/85) of patients who had a lesion on 3T-mpMRI. The anatomic delineation score was statistically significantly improved on RESOLVE (2.60 *vs* 2.68, p < .001).

DISCUSSION

In this study, we demonstrated significantly improved image quality on RESOLVE sequences compared to ss-EPI sequences for the acquisition of prostate DWI on a 3T MR scanner. With excellent interreader agreement, two experienced readers scored significantly higher image quality, less geometrical distortion and improved lesion conspicuity on RESOLVE sequences compared to ss-EPI.

DWI is the most important parameter to score peripheral zone lesions in the prostate on 3T-mpMRI. Image distortion is a major limitation in the posterior PZ areas near the rectum, interfering with lesion detection and scoring.[6] Data of the present study showed significant correlation between increment in rectal distention and geometrical distortion. When there is significant rectal distention, using alternative strategies might help improve the quality of DWI.

Figure 1. Geometrical Distortion Rankins on (a) ss-EPI, and (b) RESOLVE sequences by each reader. Score 3 and higher were considered as significant geometrical distortion. RESOLVE, Readout Segmentation of Long Variable Echo; ss-EPI, single-shot EPI.

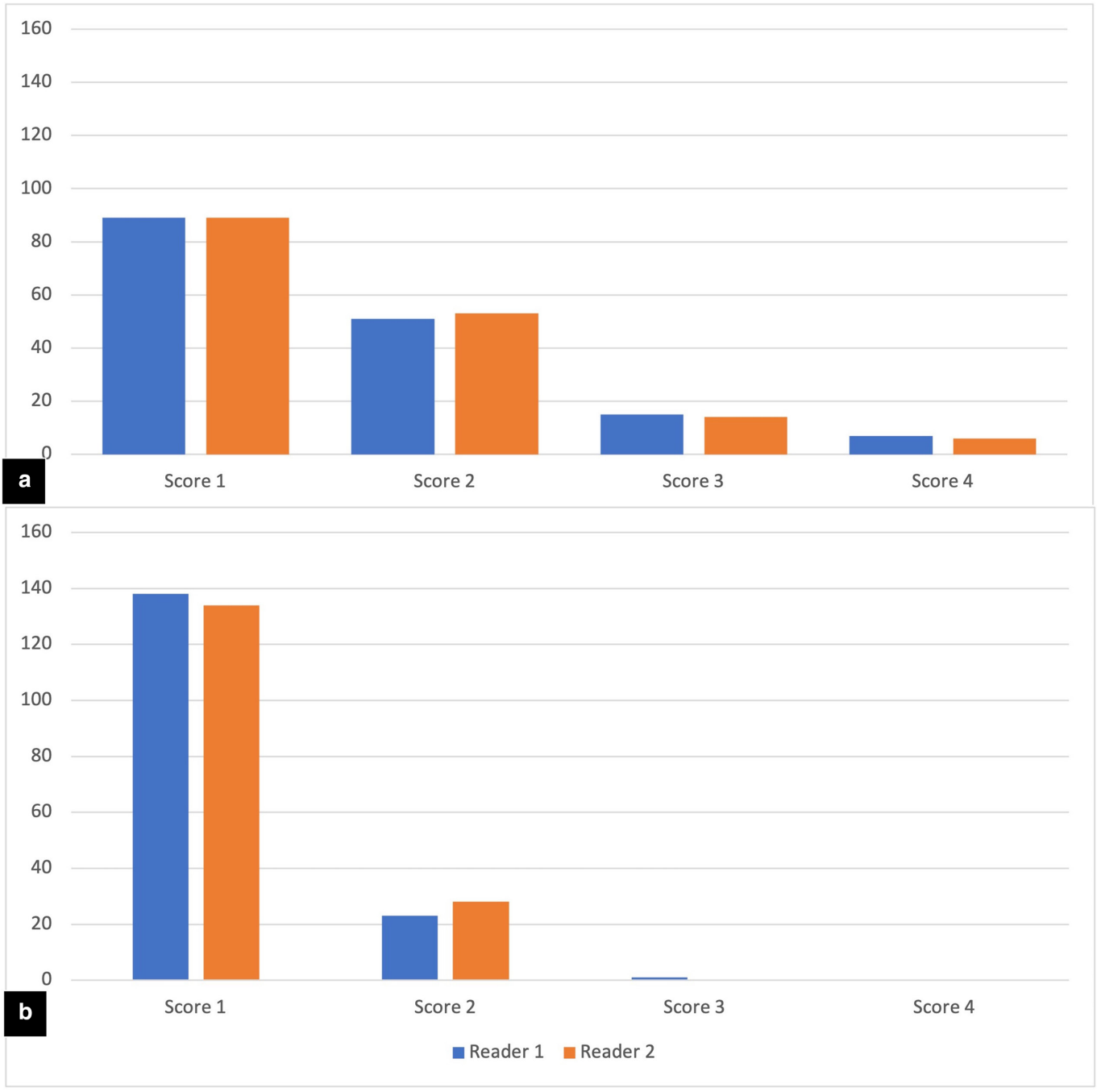

For obtaining ss-EPI, a long echo train and long TE are necessary to encode full k-space within one echo signal intensity, leading to slow k-space traversal through phase-encoding direction; ss-EPI is thus susceptible to T2* blurring and signal drop out at air–tissue interface. Furthermore, the sensitivity to susceptibility artifact increases at 3T compared to 1.5T MR scanner.[6,24] Technical improvements in image acquisition are required to enhance the diagnostic accuracy of prostate DWI at 3T scanner. In contrast to ss-EPI, rs-EPI has multi-shot EPI echo trains with segmentation in the readout direction, and the readout time of each shot is only part of the ss-EPI readout time. Subsequently, the shorter echo spacing and readout time in rs-EPI contribute to shorter effective TE and diffusion encoding time. This leads to improved image sharpness and mitigated image distortion, because the effects of susceptibility and T2* decay are reduced. This also reduces T2 shine-through effect and MR susceptibility artifact, and therefore allows better delineation of prostate abnormalities. In addition, RESOLVE incorporates a 2D navigator echo which samples the central k-space segment followed by the imaging echo train at each shot. The navigator echo data are used to identify the imaging scan that will result in unusable data and trigger a reacquisition

Figure 2. Prostate MRI in a 68-year-old male shows small-volume rectal gas (score 2) in (A) TSE *T2*-weighted and (B) dynamic contrast-enhanced T1 images. There is marked blurring and geometrical distortion of the posterior prostate peripheral zone as seen on (C, D) ss-EPI at b values of 400 and 800 s/mm^2, respectively. (Geometrical distortion score 3), with improved image quality (geometric distortion score 1), and better anatomic delineation of the prostate on corresponding (E, F) RESOLVE images at b values 50 and 800 s/mm^2. RESOLVE, Readout Segmentation of Long Variable Echo; ss-EPI, single-shot EPI; TSE, turbo spin echo.

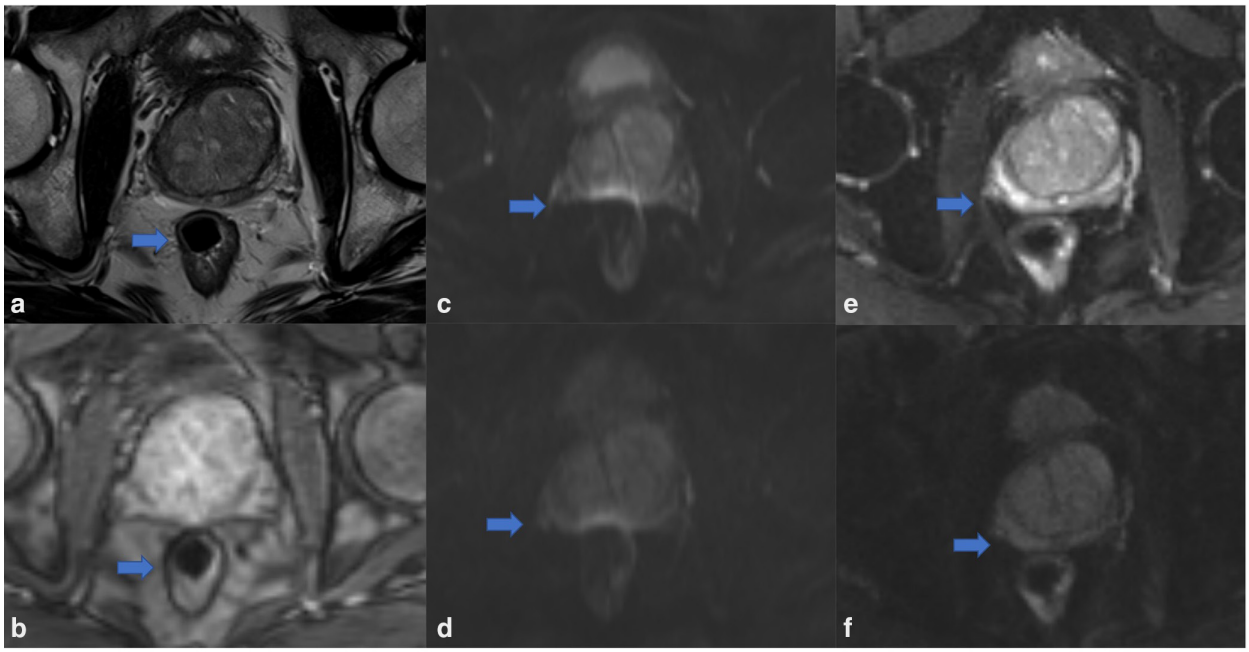

Figure 3. Prostate MRI in a 75-year-old male shows marked rectal gas (score 5) on (A) TSE *T2*-weighted, and (B) DCE images, which has caused significant (score 4) geometrical distortion on (C, D) ss-EPI at b values of 400 and 800 s/mm^2, respectively. (E, F) With RESOLVE at b values of 50 and 80 s/mm^2, respectively, there is minimal geometrical distortion (score 2) and better delineation of prostate gland boundary. DCE, dynamic contrast-enhanced; RESOLVE, Readout Segmentation of Long Variable Echo; ss-EPI, single-shot EPI; TSE, turbo spin echo.

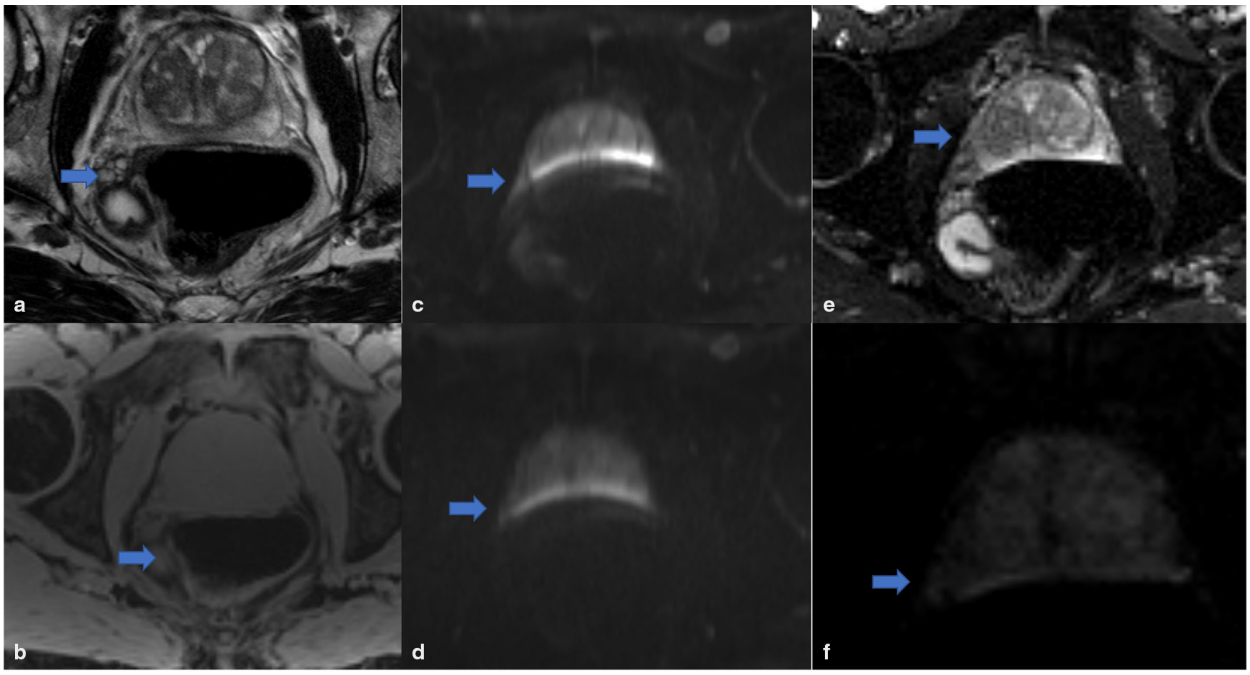

process to repeat this current scan, and to remove the shot-to-shot nonlinear phase variation in the imaging echo data during image reconstruction. These improvements are especially helpful for uncooperative patients and body parts with involuntary motion.

In this study, both readers were in excellent agreement that lesion depiction was significantly better on RESOLVE than ss-EPI. Since high b-value diffusion-weighted imaging is the primary diagnostic parameter for PIRADS v. 2.1 scoring of PZ lesions and a secondary parameter for TZ lesions, a more robust DWI sequence could improve diagnostic performance and decrease errors resulting from image artifacts. Several investigators have shown that rs-EPI outperforms ss-EPI for image quality, leading to improved lesion depiction especially in regions which are susceptible to image distortion such as orbit and skull base.[25,26] When used for the acquisition of breast DWI in a 3T MR scanner, rs-EPI has three times less geometrical distortion compared to ss-EP.[12] In a cohort of 116 patients, Li et al[27] reported outperformance of rs-EPI over ss-EPI for acquisition of prostate DWI in 90% of the study population. More recent studies have found enhanced anatomic delineation of the prostate gland, increased lesion conspicuity and improved subjective image quality with rs-EPI compared to ss-EPI, at the expense of lower SNR.[28,29] In the present study, we found significantly greater geometrical distortion on ss-EPI compared to rs-EPI. All 20 patients with geometrical distortion scores ≥ 3 on ss-EPI, had scores < 3 on rs-EPI.

A variety of image acquisition times have been reported for rs-EPI. Generally, the efficiency of rs-EPI is lower due to its segmented EPI k-space sampling trajectory compared to the single-shot k-space sampling trajectory of ss-EPI.[10] In our study, we found rs-EPI to decrease the imaging time by an average of 75 s, which were mainly attributed to the larger voxel size, fewer b-values, less averages of the rs-EPI protocol. Although having different parameters from those of the ss-EPI, using the protocols in this study, rs-EPI does not significantly affect the image acquisition time and achieved significantly improved diagnostic image quality compared to ss-EPI in terms of geometrical distortion, lesion conspicuity, and anatomic delineation. Using the protocols in this study, rs-EPI can be implemented as an alternative to ss-EPI for the acquisition of prostate DWI, without altering the total image acquisition time much. Future studies can further investigate a correlation between the acquisition time and image quality through protocol design with different acquisition times and more data acquisition for comparison. This sequence can be especially practical in patients who have a marked degree of rectal distention, which is associated with a greater amount of geometrical distortion.

Recently, there have been new diffusion techniques that could be beneficial for the image quality of prostate DWI. Single-shot turbo spin echo (ssTSE) DWI combines the benefits of SS and TSE, however, is subject to signal loss and low SNR due to phase interference. Split acquisition of fast spin-echo signals for diffusion imaging is further proposed to improve the SNR of ssTSE DWI.[30] Barth et al reported Selective-excitation accelerated reduced-FOV diffusion-weighted imaging (sTX-DWI) to fivefold shorter acquisition time compared to rs-EPI, however with significantly increased geometrical distortion.[31] In addition, reduced-FOV diffusion techniques emerged and started to be commercially available, *e.g.* ZOOMit[32] and ZOOMit^{PRO}[33] on the Siemens scanners (Siemens Healthcare, Erlangen, Germany), where the former takes advantage of the selective FOV excitation based on the dynamic parallel transmit technology and the latter excites either a smaller quadratic FOV or a reduced FOV only in the phase-encoding direction. Lacking access to these two reduced-FOV diffusion techniques due to the corresponding specific hardware and software requirements when performing data acquisition in this work, neither of them was evaluated and compared in this study. Future studies are warranted to evaluate these new reduced-FOV diffusion techniques.

While this study focused on the image quality of rs-EPI compared to ss-EPI for prostate DWI acquisition, with a large sample size and excellent interreader agreements being the strengths of the study, it was subject to several limitations. First, we did not perform any quantitative measures of image quality and SNR. Direct comparisons of SNR between ss-EPI and rs-EPI in breast and pediatric brain MRI[12,13] have shown lower SNR in rs-EPI. In contrast, some investigators have found higher SNR for rs-EPI compared to ss-EPI.[15,16] While the lower bandwidth and more efficient k-space coverage can lead to higher SNR in ss-EPI, the reduced TE in rs-EPI can increase its SNR. Second, we did not include ADC measurements in this study since inconsistent results have been reported on comparison of ADC measures between these two EPI sequences.[29] ADC measures are affected by a variety of image parameters, *e.g.* the choice of b-values, therefore comparison of ADC values without having standardized imaging parameters didn't seem to add value to the present investigation. Finally, the readers could not be truly blinded to the DWI sequence that they were evaluating, however, study results showed excellent interreader agreement between interpreters.

In conclusion, in this study, we found significantly higher DWI quality with reduced geometrical distortion on RESOLVE images compared to ss-EPI in 42% of individuals who underwent 3T-mpMRI of prostate. Using the RESOLVE sequence augments acquisition of prostate DWI by mitigating rectal gas and rectal peristalsis-related artifacts on 3T prostate mpMRI. The sequence can be an alternative or replacement of the ss-EPI diffusion sequence for the acquisition of DWI scans when there is significant geometrical distortion in ss-EPI diffusion images.

AUTHORS CONTRIBUTION

Dr. Melina Hosseiny is the primary author responsible for the integrity of the work. The work was supervised by Dr. Steven Raman and Dr. Kyung Hyun Sung. Image interpretation and analysis were performed by SR and EF. All authors have contributed to the literature review, scientific methodology, data gathering, analysis, and manuscript writing.

FUNDING

This Work Was Supported by Funds from the Integrated Diagnostics Program (IDx), Department of Radiological Sciences & Department of Pathology and Laboratory Medicine, David Geffen School of Medicine at UCLA.

REFERENCES

1. Rawla P. Epidemiology of prostate cancer. *World J Oncol* 2019; **10**: 63–89. https://doi.org/10.14740/wjon1191
2. Ahmed HU, El-Shater Bosaily A, Brown LC, Gabe R, Kaplan R, Parmar MK, et al. Diagnostic accuracy of multi-parametric MRI and TRUS biopsy in prostate cancer (PROMIS): a paired validating confirmatory study. *Lancet* 2017; **389**: S0140-6736(16)32401-1: 815–22: . https://doi.org/10.1016/S0140-6736(16)32401-1
3. Turkbey B, Brown AM, Sankineni S, Wood BJ, Pinto PA, Choyke PL, et al. Multiparametric prostate magnetic resonance imaging in the evaluation of prostate cancer. *CA Cancer J Clin* 2016; **66**: 326–36. https://doi.org/10.3322/caac.21333
4. Kasivisvanathan V, Rannikko AS, Borghi M, Panebianco V, Mynderse LA, Vaarala MH, et al. MRI-targeted or standard biopsy for prostate-cancer diagnosis. *N Engl J Med* 2018; **378**: 1767–77. https://doi.org/10.1056/NEJMoa1801993
5. Padhani AR, Weinreb J, Rosenkrantz AB, Villeirs G, Turkbey B, Barentsz J, et al. Prostate imaging-reporting and data system steering committee: PI-RADS v2 status update and future directions. *Eur Urol* 2019; **75**: S0302-2838(18)30424-X: 385–96: . https://doi.org/10.1016/j.eururo.2018.05.035
6. Mazaheri Y, Vargas HA, Nyman G, Akin O, Hricak H, et al. Image artifacts on prostate diffusion-weighted magnetic resonance imaging: trade-offs at 1.5 tesla and 3.0 tesla. *Acad Radiol* 2013; **20**: S1076-6332(13)00216-X: 1041–47: . https://doi.org/10.1016/j.acra.2013.04.005
7. Kuhl CK, Gieseke J, von Falkenhausen M, Textor J, Gernert S, Sonntag C, et al. Sensitivity encoding for diffusion-weighted MR imaging at 3.0 T: intraindividual comparative study. *Radiology* 2005; **234**: 517–26. https://doi.org/10.1148/radiol.2342031626
8. Caglic I, Hansen NL, Slough RA, Patterson AJ, Barrett T, et al. Evaluating the effect of rectal distension on prostate multiparametric MRI image quality. *Eur J Radiol* 2017; **90**: S0720-048X(17)30074-8: 174–80: . https://doi.org/10.1016/j.ejrad.2017.02.029
9. Holdsworth SJ, Skare S, Newbould RD, Guzmann R, Blevins NH, Bammer R, et al. Readout-segmented EPI for rapid high resolution diffusion imaging at 3 T. *Eur J Radiol* 2008; **65**: 36–46. https://doi.org/10.1016/j.ejrad.2007.09.016
10. Porter DA, Heidemann RM. High resolution diffusion-weighted imaging using readout-segmented echo-planar imaging, parallel imaging and a two-dimensional navigator-based reacquisition. *Magn Reson Med* 2009; **62**: 468–75. https://doi.org/10.1002/mrm.22024
11. Zhao M, Liu Z, Sha Y, Wang S, Ye X, Pan Y, et al. Readout-segmented echo-planar imaging in the evaluation of sinonasal lesions: A comprehensive comparison of image quality in single-shot echo-planar imaging. *Magn Reson Imaging* 2016; **34**: S0730-725X(15)00247-7: 166–72: . https://doi.org/10.1016/j.mri.2015.10.010
12. Bogner W, Pinker-Domenig K, Bickel H, Chmelik M, Weber M, Helbich TH, et al. Readout-segmented echo-planar imaging improves the diagnostic performance of diffusion-weighted MR breast examinations at 3.0 T. *Radiology* 2012; **263**: 64–76. https://doi.org/10.1148/radiol.12111494
13. Yeom KW, Holdsworth SJ, Van AT, Iv M, Skare S, Lober RM, et al. Comparison of readout-segmented echo-planar imaging (EPI) and single-shot EPI in clinical application of diffusion-weighted imaging of the pediatric brain. *AJR Am J Roentgenol* 2013; **200**: W437-43. https://doi.org/10.2214/AJR.12.9854
14. Tokoro H, Fujinaga Y, Ohya A, Ueda K, Shiobara A, Kitou Y, et al. Usefulness of free-breathing readout-segmented echo-planar imaging (RESOLVE) for detection of malignant liver tumors: comparison with single-shot echo-planar imaging (SS-EPI). *Eur J Radiol* 2014; **83**: S0720-048X(14)00331-3: 1728–33: . https://doi.org/10.1016/j.ejrad.2014.06.013
15. Wu C-J, Wang Q, Zhang J, Wang X-N, Liu X-S, Zhang Y-D, et al. Readout-segmented echo-planar imaging in diffusion-weighted imaging of the kidney: comparison with single-shot echo-planar imaging in image quality. *Abdom Radiol (NY)* 2016; **41**: 100–108. https://doi.org/10.1007/s00261-015-0615-5
16. Morelli J, Porter D, Ai F, Gerdes C, Saettele M, Feiweier T, et al. Clinical evaluation of single-shot and readout-segmented diffusion-weighted imaging in stroke patients at 3 T. *Acta Radiol* 2013; **54**: 299–306. https://doi.org/10.1258/ar.2012.120541
17. Iima M, Yamamoto A, Brion V, Okada T, Kanagaki M, Togashi K, et al. Reduced-distortion diffusion MRI of the craniovertebral junction. *AJNR Am J Neuroradiol* 2012; **33**: 1321–25. https://doi.org/10.3174/ajnr.A2969
18. Xia C-C, Pu J, Zhang J-G, Peng W-L, Li L, Zhao F, et al. Readout-segmented echo-planar diffusion-weighted MR for the evaluation of aggressive characteristics of rectal cancer. *Sci Rep* 2018; **8**(1): 12554. https://doi.org/10.1038/s41598-018-30488-5
19. Naganawa S, Yamazaki M, Kawai H, Sone M, Nakashima T, Isoda H, et al. Anatomical details of the brainstem and cranial nerves visualized by high resolution readout-segmented multi-shot echo-planar diffusion-weighted images using unidirectional MPG at 3T. *Magn Reson Med Sci* 2011; **10**: 269–75. https://doi.org/10.2463/mrms.10.269
20. Hara K, Watanabe H, Ito M, Tsuboi T, Watanabe H, Nakamura R, et al. Potential of a new MRI for visualizing cerebellar involvement in progressive supranuclear palsy. *Parkinsonism Relat Disord* 2014; **20**: S1353-8020(13)00362-3: 157–61: . https://doi.org/10.1016/j.parkreldis.2013.10.007
21. Rumpel H, Chong Y, Porter DA, Chan LL, et al. Benign versus metastatic vertebral compression fractures: combined diffusion-weighted MRI and MR spectroscopy aids differentiation. *Eur Radiol* 2013; **23**: 541–50. https://doi.org/10.1007/s00330-012-2620-1
22. Tanenbaum LN. Clinical applications of diffusion imaging in the spine. *Magn Reson Imaging Clin N Am* 2013; **21**: S1064-9689(12)00156-0: 299–320: . https://doi.org/10.1016/j.mric.2012.12.002
23. Thian YL, Xie W, Porter DA, Weileng Ang B, et al. Readout-segmented echo-planar imaging for diffusion-weighted imaging in the pelvis at 3T-A feasibility study. *Acad Radiol* 2014; **21**: S1076-6332(14)00008-7: 531–37: . https://doi.org/10.1016/j.acra.2014.01.005
24. Chang KJ, Kamel IR, Macura KJ, Bluemke DA, et al. 3.0-T MR imaging of the abdomen: comparison with 1.5 T. *Radiographics* 2008; **28**: 1983–98. https://doi.org/10.1148/rg.287075154
25. Wei X-E, Li W-B, Li M-H, Li Y-H, Wang D, Zhang Y-Z, et al. Detection of brain lesions at the skull base using diffusion-weighted imaging with readout-segmented echo-planar imaging and generalized autocalibrating partially parallel acquisitions. *Neurol India* 2011; **59**: 839–43. https://doi.org/10.4103/0028-3886.91361
26. Xu X, Wang Y, Hu H, Su G, Liu H, Shi H, et al. Readout-segmented echo-planar diffusion-weighted imaging in the assessment of orbital tumors: comparison with conventional single-shot echo-planar imaging in image quality and diagnostic performance. *Acta Radiol* 2017; **58**: 1457–67. https://doi.org/10.1177/0284185117695667
27. Li L, Wang L, Deng M, Liu H, Cai J, Sah VK, et al. Feasibility study of 3-T DWI of

the prostate: readout-segmented versus single-shot echo-planar imaging. *AJR Am J Roentgenol* 2015; **205**: 70–76. https://doi.org/10.2214/AJR.14.13489

28. Klingebiel M, Ullrich T, Quentin M, Bonekamp D, Aissa J, Mally D, et al. Advanced diffusion weighted imaging of the prostate: comparison of readout-segmented multi-shot, parallel-transmit and single-shot echo-planar imaging. *Eur J Radiol* 2020; **130**: S0720-048X(20)30350-8: 109161: . https://doi.org/10.1016/j.ejrad.2020.109161
29. Hellms S, Gutberlet M, Peperhove MJ, Pertschy S, Henkenberens C, Peters I, et al. Applicability of readout-segmented echoplanar diffusion weighted imaging for prostate MRI. *Medicine (Baltimore)* 2019; **98**(29): e16447. https://doi.org/10.1097/MD.0000000000016447
30. Tamada T, Ueda Y, Ueno Y, Kojima Y, Kido A, Yamamoto A, et al. Diffusion-weighted imaging in prostate cancer. *MAGMA* 2021. https://doi.org/10.1007/s10334-021-00957-6
31. Barth BK, Cornelius A, Nanz D, Eberli D, Donati OF, et al. Diffusion-weighted imaging of the prostate: image quality and geometric distortion of readout-segmented versus selective-excitation accelerated acquisitions. *Invest Radiol* 2015; **50**: 785–91. https://doi.org/10.1097/RLI.0000000000000184
32. Blasche M, Riffel P, L.M.J.M. F. (n.d.). TimTX TrueShape and syngo ZOOMit technical and practical aspects. In: *2012: Magnetom Flash*., pp. 104–34.
33 . Winkel D.J.et al., A Fully Automated, End-to-End Prostate MRI Workflow Solution Incorporating Dot, Ultrashort Biparametric Imaging and Deep- Learning-based Detection, Classification, and Reporting. 2020, Magnetom Flash. p. 78-83.